Mechanism of film growth during anodizing of Al-alloy-8090/SiC metal matrix composite in sulphuric acid electrolyte

M. SHAHID
Dr A. Q. Khan Research Laboratories, G.P.O. Box 502, Rawalpindi, Pakistan

Metal matrix composites (MMCs) consisting of Al-alloy 8090 reinforced with SiC particulate have previously proved to be susceptible to corrosion in chloride-containing environments. A study was carried out to investigate the possibility of anodizing the MMC for protection against corrosion. Sulphuric acid was found to be a preferred anodizing electrolyte for the composite, as it allowed a relatively thick anodic film to be formed on the surface. The investigation regarding the mechanism of film formation, performed on a scanning electron microscope, revealed that the thickness of the anodic film was non-uniform; however, the film–solution interface was relatively uniform compared with film–composite interface. Observation in the transmission electron microscope indicated that the pores in the anodic film which was formed, appeared round when they grew perpendicular to the surface and revealed elongated like ''finger prints'' when they developed at an angle on a rough surface, due to presence of SiC particles. The corrosion rate of the MMC, which was about 21 times the corrosion rate of ultra-pure aluminium in a chloride-containing environment, became negligible after anodizing.

1. Introduction

Metal matrix composites (MMCs) are generally susceptible to corrosion in various environments, due to either galvanic reactions between the reinforcements and the matrix, selective corrosion at the interface because of the formation of new compounds, or to the defects at the interface, causing fissures which create pathways for corrosion [1]. Therefore, MMCs are generally required to have a protective coating on the surface to enhance their corrosion resistance in hostile environments. Anodizing has been considered as a potential means of protecting MMCs with aluminium matrices, against corrosive attack, by a number of researchers [2–4]. Trzaskoma *et al.* [2] investigated the corrosion resistance of Al/SiC MMC after anodizing in sulphuric acid electrolyte, during exposure to sodium chloride solution using a.c. impedance techniques. They found that the anodized porous hardcoat significantly improved the corrosion resistance of the MMC. Aylor *et al.* [3] successfully anodized aluminium/graphite MMC in sulphuric acid and developed a 25 μm thick anodic film on the surface after anodizing for 1 h. The anodic coating on the MMC provided good corrosion protection during sea water immersion, splash and spray tests, and marine atmospheric environment test, for 180 d. Similarly, Mansfeld and Jeanjaquet [5] evaluated the corrosion resistance of SiC/Al, and graphite/Al MMCs during exposure to sodium chloride solution, before and after anodizing, using electrochemical impedance spectroscopy. Visual observation of the samples after the test did not show corrosion damage on the surface.

This paper describes the anodizing behaviour (mechanism and film morphology) and improvement in corrosion resistance after anodizing of a MMC consisting of Al-alloy 8090 reinforced with 20 wt % SiC particulate with an average particle size of 5 μm and a maximum size of 12 μm.

2. Experimental procedure

2.1. Sample preparation

A composite sheet of dimensions of 10 mm × 20 mm was polished mechanically to 1200 grit emery paper. This specimen was joined to a length of 3 mm diameter aluminium wire by crimping the composite sheet in a pre-prepared slot at one end of the wire. The joint was sealed with araldite and the aluminium wire masked with heat-shrinkable tubing. The sample material was also masked with araldite, leaving an exposed area of 1 cm^2.

2.2. Anodizing

The conventional laboratory-scale anodizing procedure was adapted. Anodizing was performed in 16 wt % sulphuric acid (88 % concentrated) using constant current densities (5–20 $mA\,cm^{-2}$) at a temperature of 23–25 °C. A flange-topped glass beaker of 1 l capacity and having five openings in the lid, was used

0022–2461

as the anodizing cell. During anodizing, the cell was immersed in a water bath to maintain a constant temperature. An annular-shaped platinum electrode with a surface area of 24 cm^2, was employed as the cathode during anodizing. A power supply (K.S.M. Herts, 4000 series) capable of supplying voltage up to 1000 V and up to 100 mA current, was used for anodizing. Agitation was provided in the electrolyte during anodizing, with the help of a glass stirrer inserted into the cell through an opening in the lid and rotated using a motor fitted on the top. A digital multimeter was used to determine the current and the potential. The current density was fixed, and the variation in voltage with time was recorded on a chart recorder. A potential divider was employed to convert the voltage sent to the chart recorder into millivolts, as high voltage would damage the chart recorder. Further details are mentioned elsewhere [8]. Samples of ultra-pure aluminium and Al-alloy 8090 were also anodized for comparison. After the anodizing, samples were taken out immediately, washed thoroughly with deionized water and dried in cold air.

2.3. Electron microscopy of anodic film

The surface morphology of the anodized specimen was studied in as-anodized form using scanning electron microscopy (SEM). For studies of the cross-section of the anodized specimen using an optical microscope and SEM, the samples were embedded in Araldite, polished to 1200 grit emery paper and lightly coated with carbon.

In order to observe the structure and morphology of porous anodic film under transmission electron microscope (TEM), a sample of the MMC was anodized at a constant current density of 25 mA cm^{-2} for 5 min and the anodic film was stripped from the substrate using the following procedure. The Araldite masking of the sample was removed and the anodized surface marked with a sharp scalpel, so that the anodic film was divided into squares of 2 mm × 2 mm. The sample was immersed in 0.1 M mercuric chloride aqueous solution contained in a shallow glass Petri dish for up to 30 min. The solution dissolved the substrate slowly and left the film floating on the surface. The stripped films were collected on copper grids (200 mesh), washed in deionized water and recollected. The film was sandwiched between two copper grids and one end of the grids was joined with Araldite to avoid them falling apart and loss of film. The stripped films were relatively thick for electron-beam penetration, therefore the sandwiched film was ion-beam thinned.

2.4. Assessment of corrosion resistance

Corrosion resistance of the anodized MMC was assessed by determining the weight loss during immersion and accelerated salt-spray tests, using near-neutral solutions containing chloride ions. For the immersion test, the anodized samples were immersed in 0.1 M sodium chloride and 0.1 M sodium sulphate solutions, contained in wide-mouthed plastic bottles. The samples were examined after every 10 d for 60 d and weighed accurately to determine any change in weight. For the salt-spray test, the samples were exposed to a spray of a near-neutral aqueous solution of high chloride and low sulphate components (0.35 % sodium chloride and 0.05 % ammonium sulphate) for 60 d. The samples were fixed on the walls of a spray cabinet at an angle of 60°. The solution was sprayed in the form of fog with the help of an atomizer. The samples were exposed to the test with 1 h wet and 1 h dry cycle and taken out of the cabinet after every 10 d to determine the change in weight. Further details of the tests are given elsewhere [6].

3. Results

3.1. Voltage–time curves

The voltage–time curves for the MMC, Al-alloy 8090 and ultra-high purity aluminium, during anodizing at a constant current density of 10 mA cm^{-2}, are given in Fig. 1. The ultra-high purity aluminium showed a rapid, approximately linear increase in voltage to 15 V in about 20 s indicating the formation of the barrier layer and pore development [7, 8]. The voltage then increased slightly, but at a decreasing rate with respect to time, before declining towards a steady state (16 V) after reaching the maximum value of 17 V. Using an anodizing ratio of 1.2–1.4 nm V^{-1} for the formation of the barrier layer on aluminium [9–11], the calculated thickness of the barrier layer was found to be about 20 nm.

In the case of the alloy 8090, the voltage increased relatively rapidly to 12 V over about 15 s; the voltage then showed a sharp decline to 10 V before gradually increasing to a steady-state voltage of about 11 V, which reached 12.5 V after 15 min. The calculated thickness of the barrier layer was about 15 nm, i.e. less than that for anodizing of ultra pure aluminium. The alloy behaviour suggests that the increased number of flaws compared with ultra-pure aluminium restricts the voltage rise probably by promoting leakage in the currents to the flaw sites; gas evolution was also observed during anodizing.

During anodizing of the MMC, the voltage increased with time at a decreasing rate until a steady-state voltage was reached after 5 min. The voltage

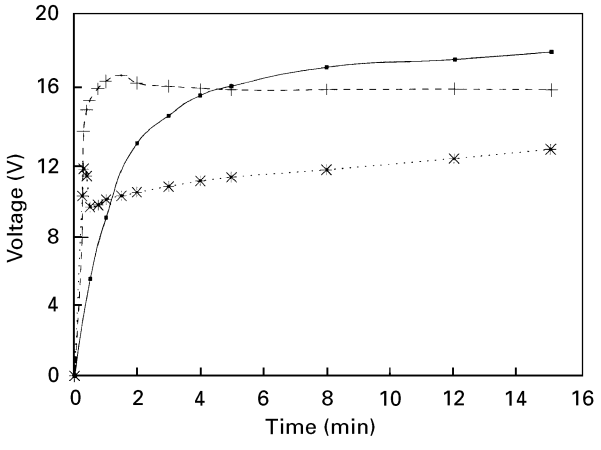

Figure 1 Voltage–time curves for various materials during anodizing in sulphuric acid, at a constant current density of 10 mA cm^{-1}. (■) Composite, (+) aluminium, (∗) Al-8090.

continued to rise, but at a relatively slow rate with time, approaching 18 V after 15 min. Therefore, the expected shape of the voltage–time curve, as revealed for ultra-pure aluminium and possibly for the alloy, was not obtained for the composite; i.e. a sharp rise in voltage up to a certain level (indicating the formation of a barrier layer) and then slight decrease followed by a steady state, was not observed. Furthermore, gas evolution (probably oxygen) was observed during anodizing at all times. Direct interpretation of the behaviour suggests that the presence of silicon carbide particles exposed to the electrolyte contributed to the behaviour. However, a relatively high steady-state voltage was eventually attained. Thus, in the early stages of anodizing the formation of porous anodic film is more difficult on the composite than aluminium, as current is lost to gas evolution.

3.2. Optical and scanning electron microscopies of anodic film

A scanning electron micrograph showing the cross-section of an anodized composite is shown in Fig. 2; the micrograph reveals the substrate supporting the anodic film. The presence of an anodic film was confirmed by its appearance and with the aid of EDX analyses in the SEM, which indicated sulphur along with aluminium when the electron beam was located within the film; oxygen was not detectable with the EDX system employed. The light regions within the anodic film are believed to be SiC particles; EDX analysis revealed silicon, but carbon could not be detected. Relatively dark regions within the cross-section of the anodic film represent cavities, which were probably generated when particles were plucked from the film during mechanical polishing of the sample for the purpose of metallography. The thickness of the anodic film was estimated to be about 20 μm. It is evident from the micrographs that the silicon carbide particles were occluded within the film during anodizing. However, a reduced number of particles are seen in the film compared with the matrix, probably due to the removal of some particles during mechanical polishing for sample preparation.

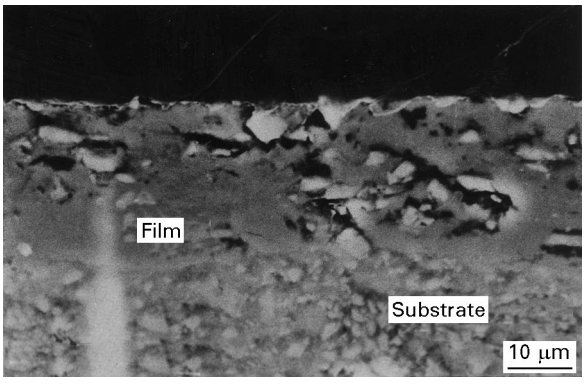

Figure 2 Scanning electron micrograph of a cross-section of anodized MMC, showing the occlusion of SiC particles within the anodic film.

Optical micrographs showing cross-sections of the anodized MMC and alloy 8090 are shown in Fig. 3a and b, respectively. It is evident from the micrographs that the anodic film formed on the composite was non-uniform in thickness (Fig. 3a), whereas the alloy supported an anodic film of uniform thickness (Fig. 3b). Fig. 3a reveals that the film–solution interface is relatively uniform, but the composite–film interface shows quite a dramatic variation in uniformity; the possible reason for this irregularity is the non-uniform distribution of silicon carbide particles in the matrix. Thicker film grows in areas of low particle density because resistance is offered to the growth of porous film by the particles. The thickness of the anodic film on the composite was in the range of 14–26 μm, whereas the alloy had an anodic film 29–30 μm thick when anodized at a current density of 10 mA cm^{-2}. The variation in the thickness of the anodic film on the composite will be discussed later.

3.3. Transmission electron microscopy of the anodic film

The morphology of stripped anodic film observed in the transmission electron microscope is shown in

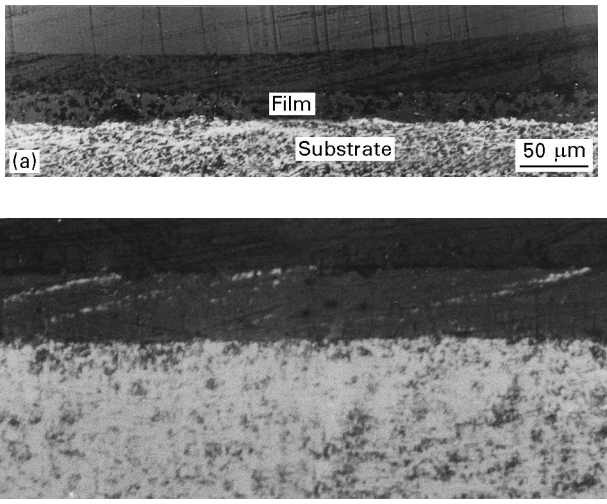

Figure 3 Optical micrographs of cross-sections of anodized (a) MMC, and (b) Al-alloy 8090, showing the film–substrate and film–solution interfaces.

Fig. 4a and b. The micrographs show the attachment of silicon carbide particles to the anodic film. It is evident that the particles were closely associated with the anodic film because, after ion-beam thinning, the particles were retained within the film and did not drop out during handling of the sample. The anodic film revealed a porous morphology, as shown in the micrographs. In some areas, pores have almost circular shapes giving a regular porous morphology (Fig. 4a); however, the majority of the anodic film consists of pores which appear as discontinuous lines forming a "finger print" network (Fig. 4b). The observations suggest that pores are round or circular, where the matrix has a relatively smooth and flat surface and pores grow perpendicular to the surface; a schematic diagram representing this type of pore formation is given in Fig. 5a. The model shows growth of porous film on a flat surface. However, the pores appear elongated where the film develops over a rough surface or where it is intersected by silicon carbide particles. This behaviour is shown schematically in Fig. 5b; pores are deflected around a particle or grow at an angle on rough surface.

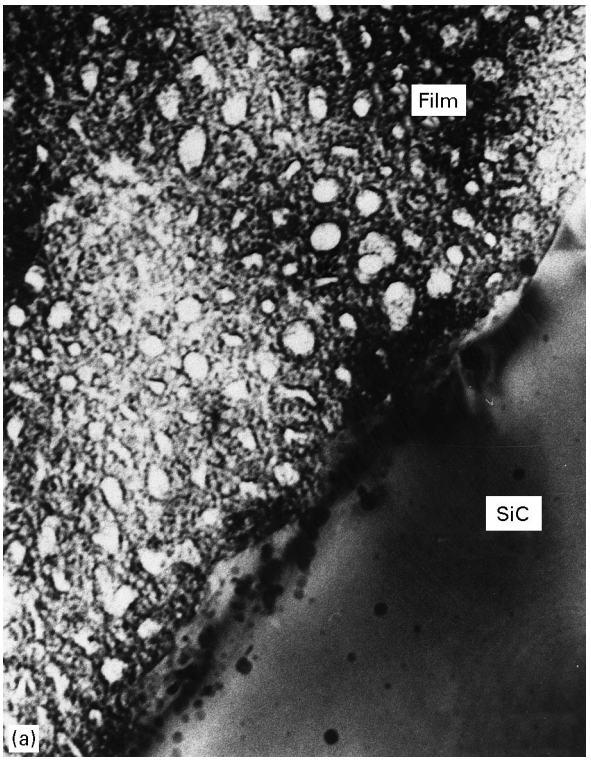

Figure 4 Transmission electron micrographs of an anodic film stripped from the composite, showing the morphology of the film, and association of SiC particles with the film. (a) ×100 000, (b) ×60 000.

3.4. Corrosion resistance of anodized samples

Fig. 6a and b show the percentage weight change as a function of time, during immersion and salt-spray tests, respectively. For comparison, anodized samples of pure aluminium and the alloy 8090 were also exposed to the tests. All three materials did not show any significant change in the weight even after 60 d exposure to the tests. Rather, the samples showed a slight gain in weights which was probably due to absorbed water/moisture by Araldite resin used to mask the non-anodized surface during anodizing and the tests. Scanning electron microscopy of the samples exposed to the tests revealed no significant change in the surface appearance. Previous study revealed that the corrosion rate of the composite was 21 times and that of the alloy was 7 times the corrosion rate of the ultra-pure aluminium, after 60 d immersion in similar solution. Similarly, after 60 d exposure to the salt-spray test, the alloy showed a corrosion rate 3 times that of the ultra-pure aluminium whereas the corrosion rate

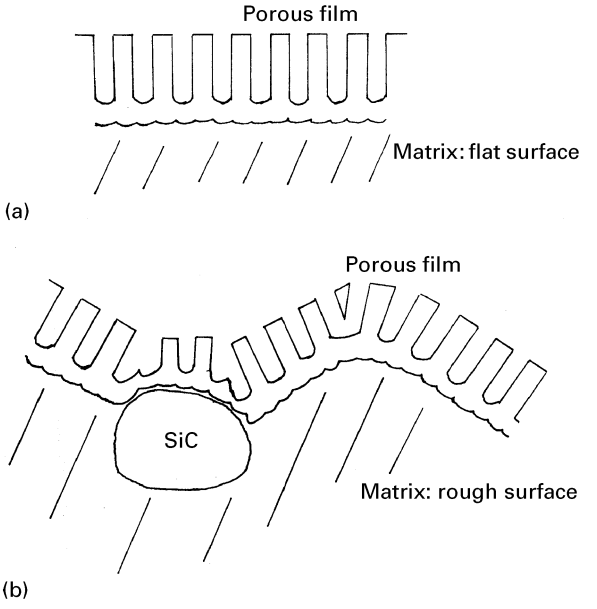

Figure 5 Schematic diagrams showing growth of porous anodic film on the matrix of the composite at (a) a flat surface and (b) a rough surface, with SiC.

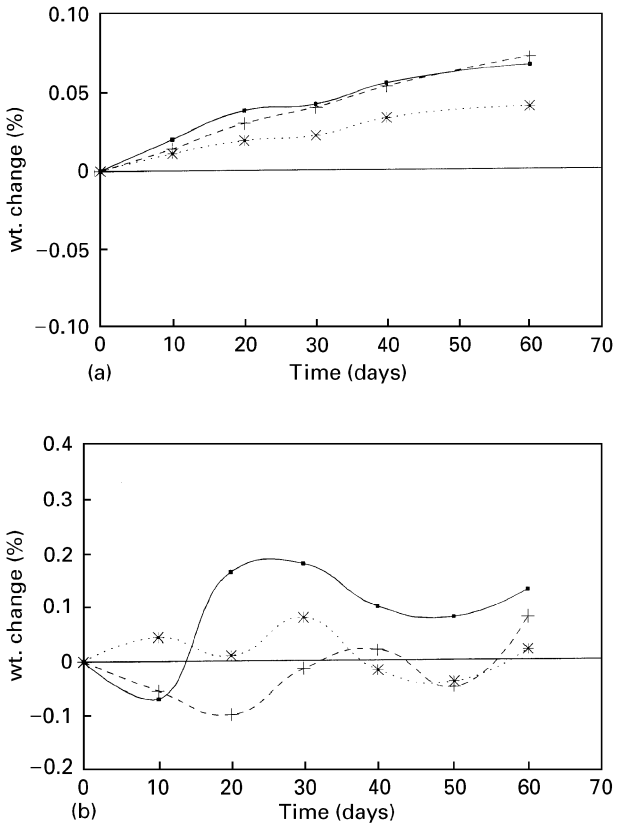

Figure 6 Percentage weight loss data of various anodized materials as a function of time during (a) the immersion test, and (b) the salt-spray test. (■) composite; (+) Al-8090; (✳) Al.

of the composite was 14 times that of the aluminium [6]. This indicates a significant improvement in the corrosion resistance of the alloy and the composite after anodizing.

4. Discussion

The composite developed a relatively thick anodic film during anodizing in sulphuric acid, as is evident from micrographs of the cross-sections of the anodized specimen (Figs 2 and 3a). It is of interest to postulate mechanisms of film growth on the MMC, with the aid of observations made during scanning and transmission electron microscopy of the anodic film. Cooke's study [12] of the development of defects in the anodic film resulting from the presence of intermetallic compounds, was also helpful in this regard. Keeping in view the experimental observation and the Cook's model. a schematic illustration of anodic film formation on MMC containing an individual silicon carbide particle is given in Fig. 7a–d; Fig. 7a shows a polished cross-section containing a particle buried in the matrix. A pre-existing air-formed film is present on the adjacent matrix. Silicon carbide particles are poor electrical conductors and due to their high electrical resistance, current will tend to concentrate in the matrix around the particles consuming the surrounding aluminium, which will result in the situation shown in Fig. 7c. The growth of pores in the area adjacent to the particle is shielded by the particle and the pores, instead of growing perpendicular to the

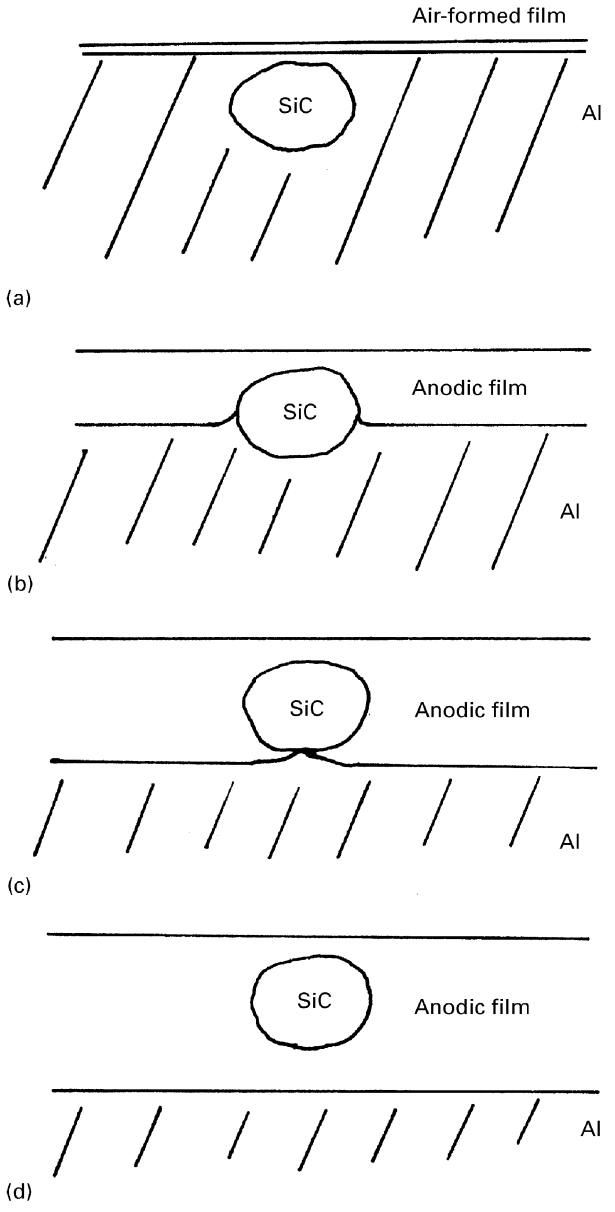

Figure 7 Schematic diagrams showing the occlusion of an SiC particle (fully embedded in the matrix) within the anodic film, during anodizing.

macroscopic metal surface, grow around the particle; this is evident from the transmission electron micrographs of stripped anodic film, shown in Fig. 4a and b. As the anodic film grows, the metal–oxide interface recedes from the vicinity of the particle (Fig. 7c). Continuation of anodizing causes the cone of aluminium under the particle to form a porous film and, consequently, the particle is completely occluded within the anodic film, as shown in Fig. 7d; the complete occlusion of the silicon carbide particles within the anodic film is evident from Fig. 2. During anodizing of the matrix, when the pores are shielded by the particles, some of them are terminated while others are deflected and branched, growing around and at the sides of the particle initiating the process of occlusion. The deflection of pores around a silicon carbide particle is shown schematically in Fig. 8. The schematic models show the mechanism of porous anodic film formation on the matrix containing one particle; however, in the real situation, the matrix contains numerous particles

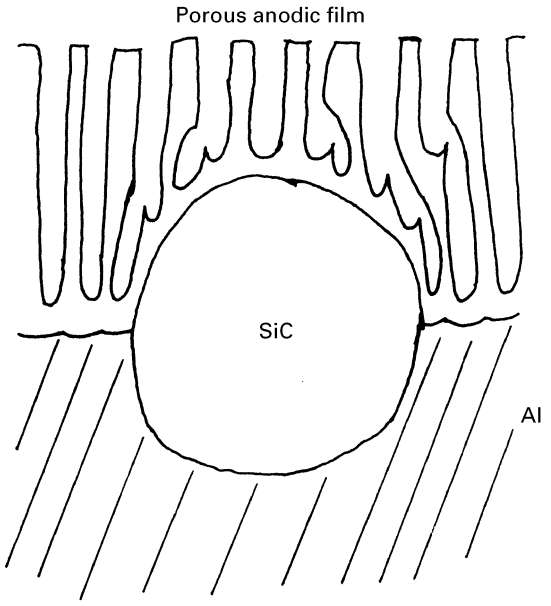

Figure 8 Schematic diagram showing the deflection of pores around an SiC particle during anodizing.

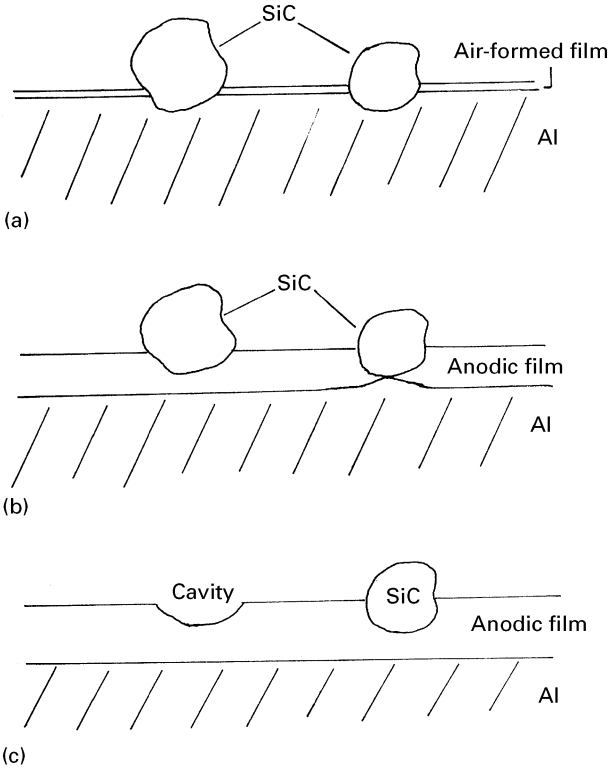

Figure 9 Schematic diagrams showing the occlusion of an SiC particle (semi-buried in the matrix) within the anodic film and the formation of a cavity on the surface of the film due to removal of the particle.

having various shapes and sizes and lying in different planes.

A further situation arises when a particle is partially buried in the matrix, as shown schematically in Fig. 9a. Growth of anodic film on the matrix takes place by the mechanism discussed previously. As shown in Fig. 9b, the particle having a smaller volume buried in the matrix is occluded readily within the anodic film, however, the particle half-buried in the matrix is still in the process of occlusion. During anodizing, as the electrolyte is agitated continuously, the chances for removal of the particles now present on the surface of the anodic film are predominant, which produces cavities on the surface of the anodic film.

The particles which are on the surface of the substrate before anodizing are contained on the surface of the anodic film after anodizing, or leave the anodic film and produce cavities. The particles within the anodic film, however, remain within the film and form an integral part of the film. The nonuniformity in film thickness is attributed to the surface roughness of the composite (the surface was mechanically polished before anodizing), and to the non-uniform distribution of the silicon carbide particles. Thicker film formation takes place on the ridges present on the surface as investigated by Thompson *et al.* [13]. The film thickness is assumed to be restricted where there is a relatively high population density of the silicon carbide particles, because the silicon carbide particles provide shielding of the matrix.

The examination of the stripped anodic film from the surface of the composite in the TEM reveals the presence of silicon carbide particles within the anodic film (Fig. 4a, b). The silicon carbide particles are surrounded by the anodic film; this is further evidence of occlusion of particles within the film. At relatively low magnification, the porous anodic film stripped from the matrix reveals the pores, giving a "finger print" impression (Fig. 4b); pores of circular section, irregular shape and in the form of discontinuous lines are revealed. The circular pores represent the expected morphology of the porous anodic film and the pores of irregular shapes arise due to the shielding of the matrix by the silicon carbide particles, causing the pores to grow around the particles. The discontinuous lines represent the pores which are deflected when the silicon carbide particles are approached. Thompson *et al.* [14] observed a similar morphology during anodizing of aluminium-containing intermetallic particles in sulphuric acid electrolyte.

In the present study it is evident that the MMC can be successfully anodized using sulphuric acid electrolyte; although some resistance is offered by the silicon carbide particles which do not themselves take part in the process but rather cause hindrance. The surfaces of the anodic films were not degraded after the corrosion tests, as is evident from Fig. 6a and b. Therefore, on the basis of these tests it can be suggested that the corrosion resistance of the composite was improved by anodizing, which indicates that the components made of the MMC can be used in hostile environments after anodizing.

5. Conclusions

1. The composite can be anodized in sulphuric acid and a sufficiently thick anodic film is formed; the silicon carbide particles are occluded within the film forming an integral part of it.

2. The thickness of the anodic film formed on the surface is not uniform; the film–solution interface is

relatively uniform compared with the film–composite interface. This is believed to be due to the non-uniform distribution of the particles in the matrix.

3. Pores of the anodic film formed on the matrix appear round when they are viewed perpendicular to the surface; they appear elongated when they develop at an angle on a rough surface or are shielded by the particles.

4. The anodic film formed in sulphuric acid can afford corrosion resistance to the composite when exposed to hostile environments containing chloride and sulphate species.

Acknowledgement

This research was carried out at the Corrosion and Protection Centre, University of Manchester Institute of Science and Technology (UMIST), Manchester, UK.

References

1. M. METZGER and S. G. FISHMAN, *Ind. Eng. Chem. Prod. Res. Dev.* **22** (1983) 296.
2. P. P. TRZASKOMA, E. McCAFFERTY and C. R. CROWE, *J. Electrochem. Soc.* **130** (9) (1983).
3. D. M. AYLOR, R. J. FERRARA and R. M. KAIN, *Mater. Performance*, July (1984) 32.
4. D. M. AYLOR and R. M. KAIN, in "Recent advances in composites in USA and Japan", ASTM STP 846, edited by J. R. Vinson and M. Taya (American Society for Testing and Materials, Philadelphia, PA, 1985) p. 997.
5. F. MANSFELD and S. L. JEANJAQUET, *Corros. Sci.* **26** (9) (1986) 727.
6. M. SHAHID, PhD thesis, University of Manchester Institute of Science and Technology, UK (1991).
7. G. E. THOMPSON *et al. Nature* (Lond.) **272** (1978) 511.
8. C. E. ALVEY, G. C. WOOD and G. E. THOMPSON, in "Proceedings of the 10th World Congress on Metal Finishing", edited by S. Hanuyama (1980) p. 275.
9. A. J. BROCK, MSc dissertation, University of Manchester (1963).
10. S. J. BASINKA, J. POLLING and A. CHARLESBY, *Acta Metall.* **2** (1954) 313.
11. M. S. HUNTER, *Electrochem. Technol.* **1** (1963) 151.
12. W. E. COOKE, *Plating*, **49** (1962) 1157.
13. G. E. THOMPSON *et al. Nature* (Lond.) **272** (1978) 433.
14. G. E. THOMPSON, R. C. FURNEAUX and G. C. WOOD, *Trans. IMF* **55** (1977) 117.

Received 31 October 1995
and accepted 10 February 1997